CrossMark

Influence of Supports on Pd Catalysts for the Selective Catalytic Reduction of NO_x with H_2 and CO

Gianni Caravaggio[1] · **Lioudmila Nossova**[1] · **Raymond Burich**[1]

© Her Majesty the Queen in Right of Canada 2015

Abstract A major concern of current commercial catalysts for the selective catalytic reduction (SCR) of nitrogen oxides (NO_x) (DeNO$_x$) is the lack of sufficient catalytic activity at low temperatures (below 200°C) that typically occur during cold start and urban driving conditions. To address this issue, a study was undertaken to develop an (H_2 + CO)-SCR Pd-based catalyst to obtain high DeNO$_x$ activity in this low-temperature range. A series of catalysts with Pd loaded on supports containing various amounts of γ-alumina (γ-Al$_2$O$_3$) (0–65 wt%), CBV-2314 (15–100 wt%), and TiO$_2$ (0–20 wt%) were tested for DeNO$_x$ activity and aging in a catalyst testing unit (CTU). The results showed that each component in the support played a role in the NO_x conversion, depending on the temperature. Catalysts with Pd supported on {[γ-Al$_2$O$_3$ (60 wt%)+CBV-2314 (20 wt%)]–TiO$_2$ (20 wt%)} achieved the best overall DeNO$_x$ activity. Catalysts with various Pd loadings (0.05 wt% to 0.5 wt%) were prepared with a {[γ-Al$_2$O$_3$ (60 wt%)+CBV-2314 (20 wt%)]–TiO$_2$ (20 wt%)} support. The catalysts loaded with 0.05 wt% and 0.2 wt% Pd demonstrated the best overall DeNO$_x$ activity (up to 90 % NO_x conversion starting at 150 °C). These catalysts were subjected to an accelerated aging regime. Based on the aging studies, the 0.2 wt% Pd/{[γ-Al$_2$O$_3$ (60 wt%)+CBV-2314 (20 wt%)]–TiO$_2$ (20 wt%)} composition was the most active and stable catalyst.

Keywords NO_x/H_2/CO · Palladium catalyst · Promoter · γ-Al$_2$O$_3$–CBV-2314–TiO$_2$ · Catalyst aging

✉ Gianni Caravaggio
   gianni.caravaggio@canada.ca

[1] Natural Resources Canada, CanmetENERGY, 1 Haanel Drive, Ottawa, Ontario K1A 1M1, Canada

1 Introduction

Diesel engine exhaust contains many components that are hazardous to human health [1] and are also detrimental to the environment. Of primary concern are the nitrogen oxides (NO_x) since they cause acid rain and ground-level ozone. In 2009, the transportation sector accounted for 60 % of all NO_x emissions, and as a result, stricter regulations especially for diesel engines have been implemented, prompting further research for new technologies to reduce these emissions [1].

Diesel engines have the advantage of being more efficient than gasoline engines, and their widespread use could offer a significant reduction of greenhouse gases (GHGs) from the transportation sector. However, the reduction of NO_x from diesel engines functioning in lean burn conditions is difficult due to the large excess of oxygen present in the exhaust. To address this issue, improvements to diesel engine design and operation regimes have been implemented. For some diesel vehicles, aftertreatment systems have been successfully installed to meet present environmental regulations. However, reducing NO_x emissions at low temperatures is still problematic [2] and future more stringent regulations will require more advanced technologies for NO_x emission reduction.

Significant attention has been given to the development of selective catalytic reduction (SCR) of NO_x using H_2 [3–18], CO [19–21], or a mixture of H_2/CO [22–33] as reductant. Catalysts using H_2 and/or CO have the advantage of low-temperature DeNO$_x$ activity, and the reductants could be produced using an on-board fuel reformer, thus eliminating the need of carrying any additional reductant.

Many of the catalysts for NO_x reduction using H_2 as a reductant employ platinum as the active metal. These catalysts show high DeNO$_x$ activity at low temperatures but suffer from

CO poisoning resulting in a decrease in catalytic activity, and they also tend to produce large amounts of N$_2$O, a potent GHG [34–36]. Nevertheless, some improvements have been made in CO tolerance for Pt-type catalysts as indicated in two studies using catalysts of Pt/WO$_3$/Zr and Pt/MCM-41 [6, 8]. However, in both cases, reduced conversion was obtained in the presence of more than 100 ppm of CO.

In contrast, the use of palladium (Pd) is an attractive alternative since it has shown enhanced reactivity toward the selective reduction of NO$_x$ in the presence of CO [23, 32, 35]. Previous research typically focused on catalysts with Pd loaded on Al$_2$O$_3$ (alumina), TiO$_2$ (titania), or mixtures of Al$_2$O$_3$–TiO$_2$ supports [10, 12, 13, 22, 29, 30, 32, 33, 37]. Macleod et al. demonstrated that catalysts containing Pd and using H$_2$ or combined H$_2$ and CO as reductants had high NO$_x$ conversion in the low to medium-temperature range (~125 to 300 °C) [30, 32, 37]. The studies also showed that the Pd/Al$_2$O$_3$–TiO$_2$ catalyst had higher catalytic activity than those with alumina or titania alone and they attributed this to a synergy between the two supports [30]. Konsolakis et al. [29] and Greenhalgh et al. [22] showed that the addition of promoters to Pd catalysts resulted in improved conversion. High NO$_x$ conversion (80–100 %) and high N$_2$ selectivity (80–90 %) have also been demonstrated with Pd/Al$_2$O$_3$ and V$_2$O$_5$. However, V$_2$O$_5$ is toxic and its release into the environment should be avoided [10, 12]. Catalysts with Pd loaded on pillared clays [26], on zeolites (MFI, beta zeolite) [15], and on perovskite structures showed good NO$_x$ conversion (80–100 %) and N$_2$ selectivity (40–60 %) [3, 5]. Other metals such as iridium (Ir/Ba/ WO$_3$/SiO$_2$) [20] and silver (Ag/Al$_2$O$_3$) [24] have also been investigated for the reduction of NO$_x$ using H$_2$ or H$_2$ and CO as reductants. However, not all studies mentioned above used water in the testing gas feed, a major component of diesel exhaust [3, 7, 10–15, 17, 18, 21, 23, 29–33, 38], and in many cases, when water was present, the catalysts showed a decrease in DeNO$_x$ activity [4, 5, 7, 8, 20, 26–28, 39].

The aim of this study was the development of a H$_2$/CO SCR catalyst displaying marked low-temperature activity and expanded DeNO$_x$ temperature range performance in the presence of water. The catalysts studied were palladium loaded on supports consisting of mixtures of γ-alumina, CBV-2314 (an ammonium ZSM-5-type zeolite with a silica to alumina ratio of 23:1) that were coated with TiO$_2$ in the following ranges: γ-alumina (0–65 wt%), CBV-2314 (15–100 wt%), and TiO$_2$ (0–20 wt%). Pd loadings were varied to minimize metal content and to maximize DeNO$_x$ activity. The best catalysts were aged and tested for DeNO$_x$ activity. All the catalysts were tested using a simulated diesel engine exhaust stream that contained water.

2 Experimental

2.1 Catalyst Preparation

2.1.1 Supports

The catalyst supports were prepared by combining γ-Al$_2$O$_3$, CBV-2314, and TiO$_2$ in various ratios. γ-Al$_2$O$_3$ was prepared by a sol–gel method, CBV-2314 (ZSM-5 zeolite) was purchased from Zeolyst International, and TiO$_2$ was generated from Ti^{4+} isopropoxide (Sigma-Aldrich, 97 % purity). The details of the synthesis are described below.

Preparation of γ-Al$_2$O$_3$ High-surface-area γ-alumina was prepared by using a modified sol–gel method [40]. 2-Methylpentane-2,4-diol (120 g) was mixed with aluminum isopropoxide (108 g) and stirred for 4 h at 120 °C. After lowering the temperature to 100 °C and adding 90 ml of de-ionized water, the mixture was stirred vigorously for 2 h, and then, it was left to stir overnight at 80 °C. The resulting slurry was dried under vacuum using a rotary evaporator and then placed in an oven overnight at 120 °C. The subsequent γ-Al$_2$O$_3$ product was calcined at 500 °C for 6 h in air.

Preparation of (γ-Al$_2$O$_3$–TiO$_2$), CBV-2314–TiO$_2$, and (γ-Al$_2$O$_3$ + CBV-2314)–TiO$_2$ Supports The mixed supports were prepared by depositing TiO$_2$ on γ-Al$_2$O$_3$ + CBV-2314, CBV-2314, or γ-Al$_2$O$_3$. To carry out the TiO$_2$ deposition, titanium isopropoxide was hydrolyzed in the presence of the support. Three different types of supports were prepared: γ-Al$_2$O$_3$–TiO$_2$, CBV-2314–TiO$_2$, and (γ-Al$_2$O$_3$ + CBV-2314)–TiO$_2$. The resulting mixtures were dried at 120 °C for a minimum of 4 h then calcined at 500 °C for 6 h in air.

2.1.2 Catalysts

The catalysts were prepared by adding palladium (palladium(II) nitrate, 99.9 %, Alfa Aesar) to the above supports by the incipient wetness impregnation procedure using an aqueous solution of Pd(II) nitrate to produce metal loadings of 0.05 wt%, 0.2 wt%, and 0.5 wt% loading of metal. Subsequent to the impregnation, the catalysts were dried at 120 °C for ~16 h and calcined at 500 °C for 6 h in air.

2.2 Catalyst Characterization and Testing

2.2.1 Composition

Catalyst compositions were determined using a Hitachi S3400N VP-SEM with an Oxford INCA energy-dispersive X-ray (EDX) detector system operating at 20 kV and 80–90 mA. A thin layer of powder catalyst was deposited and held in place on a double-sided carbon tape. The excess was

12

Emiss. Control Sci. Technol. (2016) 2:10–19

blown off with a gentle stream of nitrogen. For each catalyst, ten random locations, chosen by the INCA automation software, were analyzed. Average and standard deviation of the measurements were calculated to determine the final composition of the catalysts.

2.2.2 BET Surface Area

The surface area of the samples was determined by the Brunauer–Emmett–Teller (BET) method using a Micromeritics ASAP 2010 surface area and porosity analyzer. Each sample was degassed at 250 °C for 16 h, and the isotherms were measured by standard nitrogen adsorption at −196 °C.

2.2.3 Pd Dispersion by Hydrogen–Oxygen Titration

The Pd metal dispersion was determined by a hydrogen–oxygen titration method using a Micromeritics ASAP 2020C instrument. Prior to adsorption experiments, catalysts were first pretreated in helium flow at 350 °C for 2 h, and then, they were reduced in situ in hydrogen flow at 350 °C for 2 h followed by evacuation for 30 min until a pressure of 5 μm of Hg was reached. This pretreatment removed all impurities from the sample and produced a catalytically active surface of palladium. When the catalyst was cooled to 35 °C, oxygen adsorption at this temperature was performed according to the reaction (surface palladium atoms (Pd_S)):

$$Pd_S + 1/2 O_2 \rightarrow Pd_S\text{-}O$$

After evacuation at 35 °C for 30 min, the next titration of chemisorbed oxygen by hydrogen was performed at 35 °C according to the following equation:

$$Pd_S\text{-}O + 3/2 H_2 \rightarrow Pd_S\text{-}H + H_2O$$
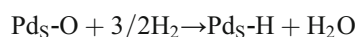
Hydrogen uptake during titration was determined using the same static volumetric method as for hydrogen chemisorption. In this method, a known amount of hydrogen was dosed and subsequently adsorbed at different partial pressures resulting in a chemisorption isotherm five points from 130 to 270 mm of Hg. This isotherm measurement was repeated after an evacuation step at the analysis temperature. The repeat isotherm represented weakly adsorbed species. The difference between the initial and repeat isotherms resulted in the chemisorbed amount of hydrogen. Metal dispersion was calculated by linear extrapolation of the difference isotherm to zero pressure. The results were expressed as the ratio of the number of mol of hydrogen chemisorbed to the number of mol of Pd in the catalyst based on the adsorption stoichiometry factor (Pd_s/H_2) of 2/3. A ratio of 1.00 is defined as 100 % dispersion D_M ($D_M = N_S^M / N_T^M$, surface atoms of metal/total atoms of metal).

2.2.4 NOx Reduction Activity

The catalysts were tested in a fixed bed flow reactor system consisting of a vertical quartz tube enclosed in a temperature-controlled furnace. Each sample was ground to a fine powder and then pressed into thin (ca. 16-mm dia.) wafers under 7 t of force. After lightly crushing these wafers in a mortar and pestle, the particles were sieved within a size range of 80 to 120 mesh. The particles (~500 mg) were then loaded into a quartz reactor tube (6.12-mm nominal ID by 40.64 cm long) yielding a typical catalyst bed height of 26 mm. All catalytic experiments were conducted at a gas hourly space velocity (GHSV) ~95,000 h^{-1} [standardized to 20 °C and 1 atm] based on the catalyst volume minus the volume occupied by the thermocouple. The operating parameters were as follows: GHSV ~95,000 h^{-1}; the temperature was ramped from 75 to 600 °C at 3 °C/min; and the feed gas composition was 500 ppm NO, 5 % O_2, 5 % H_2O, 0.3 % H_2, 0.1 % CO, and the balance He. A test was also conducted to determine the effect of CO_2 on catalyst activity by using the same simulated diesel exhaust with the addition of 7.5 % CO_2. The 3:1 H_2/CO ratio was used for the reductant since it was determined to be the optimum value for catalytic activity. However, a typical H_2/CO ratio of 1:3 is found in engine exhaust under normal operating conditions [41]. Therefore, an additional source of H_2 would be needed to achieve the 3:1 H_2/CO ratio that was used in this study. A full description of the testing system was published by Greenhalgh et al. [22].

2.2.5 Catalyst Aging

The catalysts were aged at three different temperatures using the same simulated diesel engine exhaust composition as for the activity test. The aging parameters are shown in Table 1. After each aging cycle, the catalysts were tested for DeNO$_x$ activity using the regular testing procedure. It is difficult to estimate if aging conditions are severe enough to meet target applications for a diesel engine. However, the aging procedure used in this work was harsher than the procedure from a paper by Komatsu et al. [41] that estimated aging at 750 °C for 24 h corresponded to 80,000-km usage on a diesel vehicle.

Table 1 Aging parameters

Aging cycle	Temperature (°C)	Duration (h)
1	650	6
2	750	10
3	750	18

Table 2 Nominal composition of Pd catalysts prepared with supports containing various amounts of γ-Al$_2$O$_3$, CBV-2314, and TiO$_2$

Catalyst notation Pd/(x+y)−z	Nominal catalyst support composition (wt%)			Pd loading (wt%)
	x γ-Al$_2$O$_3$	y CBV-2314	z TiO$_2$	
Pd/(0+100)−0	0	100	0	0.2
Pd/(0+80)−20	0	80	20	0.2
Pd/(80+0)−20	80	0	20	0.2
Pd/(60+20)−20	60	20	20	0.2
Pd/(60+25)−15	60	25	15	0.2
Pd/(60+30)−10	60	30	10	0.2
Pd/(50+30)−20	50	30	20	0.2
Pd/(65+15)−20	65	15	20	0.2
Pd/(70+10)−20	70	10	20	0.2

3 Results and Discussion

3.1 Composition and Surface Area

Table 2 shows the nominal composition and names of each catalyst in the form of Pd/(x+y)−z where x, y, and z stand for γ-Al$_2$O$_3$, CBV-2314, and TiO$_2$, respectively. Table 3 shows the elemental composition (wt%) of the catalysts, as determined by SEM/EDX. Measured and nominal ratios of the components (Si/Al, Si/Ti, and Al/Ti) are shown in Table 4. The small variation between the measured and nominal atomic ratios was taken to be confirmation that the supports had the expected amount of each component (γ-Al$_2$O$_3$, CBV-2314, and TiO$_2$). The palladium concentrations were in the same order of magnitude as that of the nominal loading, indicating that the incipient wetness procedure was successful and the correct amount of metal was added to the support. Furthermore, since the support was made up of the combination of three components, it was likely that a larger fraction of the Pd will be loaded on the component of the support with a higher pore volume (i.e., γ-Al$_2$O$_3$ which has the largest pore volume, Table 5).

The BET surface areas (SAs), pore volumes, and average pore sizes of the catalysts and supports are presented in Table 5. Calcined commercial CBV-2314 and γ-Al$_2$O$_3$ had SAs of 342 and 290 m^2/g, respectively. The SA of the Pd/(0+100)−0 (Pd on CBV-2314) catalyst is within 6 % of the pure calcined CBV-2314 indicating that there are no structural changes of the original material. In contrast, the Pd/(0+80)−20 catalyst had significantly lower SA than calcined CBV-2314 (ca. 286 m^2/g vs. 342 m^2/g, respectively). The SA of Pd/(80+0)−20 was also lower than that of pure γ-Al$_2$O$_3$ (ca. 251 m^2/g vs. 290 m^2/g, respectively). The decreases in SA appeared to be due to the dilution of CBV-2314 and γ-Al$_2$O$_3$ with TiO$_2$. There was no significant difference between the SAs of the γ-Al$_2$O$_3$-containing catalysts (SAs varying between 251 and 297 m^2/g). These SAs were similar to that of pure γ-Al$_2$O$_3$, the major component of the support, indicating that the structures were not affected by the addition of

Table 3 Composition by SEM/EDX of Pd catalysts prepared with supports containing various amounts of γ-Al$_2$O$_3$, CBV-2314, and TiO$_2$

Catalyst notation	Catalyst composition (wt%)				
	Al	Si	Ti	Pd	O
Pd/(0+100)−0	3.52	43.30	0.00	0.29	52.61
Pd/(0+80)−20	2.77	33.64	13.47	0.26	49.85
Pd/(80+0)−20	40.36	0.00	14.05	0.27	45.32
Pd/(60+20)−20	29.95	8.85	14.38	0.20	46.51
Pd/(60+25)−15	29.25	12.69	10.27	0.27	47.46
Pd/(60+30)−10	29.04	15.41	7.06	0.26	48.19
Pd/(50+30)−20	24.42	14.65	13.30	0.23	47.37
Pd/(65+15)−20	32.85	7.56	12.87	0.22	46.47
Pd/(70+10)−20	35.72	4.80	13.20	0.21	46.09

Table 4 Calculated and SEM/EDX atomic ratios for catalysts

Catalyst notation	Calculated atomic ratio					
	From nominal			From SEM/EDX		
	Si/Al	Si/Ti	Al/Ti	Si/Al	Si/Ti	Al/Ti
Pd/(0+100)−0	11.5	NA	NA	11.8	0.0	0.0
Pd/(0+80)−20	11.5	5.0	0.4	11.7	4.3	0.4
Pd/(80+0)−20	NA	NA	6.3	0.0	0.0	5.1
Pd/(60+20)−20	0.3	1.2	4.8	0.3	1.0	3.7
Pd/(60+25)−15	0.3	2.1	6.5	0.4	2.1	5.1
Pd/(60+30)−10	0.4	3.7	9.7	0.5	3.7	7.3
Pd/(50+30)−20	0.5	1.9	4.1	0.6	1.9	3.3
Pd/(65+15)−20	0.2	0.9	5.2	0.2	1.0	4.5
Pd/(70+10)−20	0.1	0.6	5.5	0.1	0.6	4.8

NA not applicable

14

Emiss. Control Sci. Technol. (2016) 2:10–19

Table 5 Textural properties of catalysts

Catalyst support notation	BET surface area (m²/g)	Pore volume (cm³/g)[a]	Average pore size (Å)[b]
γ-Al$_2$O$_3$	290	1.11	153
CBV-2314	342	0.19	22
Pd/(0+100)−0	363	0.20	22
Pd/(0+80)−20	286	0.18	26
Pd/(80+0)−20	251	0.96	158
Pd/(60+20)−20	290	0.61	85
Pd/(60+25)−15	271	0.41	62
Pd/(60+30)−10	297	0.52	70
Pd/(50+30)−20	275	0.41	60
Pd/(65+15)−20	270	0.61	90
Pd/(70+10)−20	269	0.65	97

[a] Single point adsorption total pore volume of pores

[b] 4V/SA where V is the total pore volume and SA is the BET-specific surface area

TiO$_2$ or Pd and confirming that TiO$_2$ was finely dispersed on the surface of γ-Al$_2$O$_3$ support [30]. As expected, the Pd/(0+100)−0 catalyst with a pure zeolite support had a higher SA than the other γ-Al$_2$O$_3$-containing catalyst.

3.2 DeNO$_x$ Activity

In order to determine the support composition with the optimum DeNO$_x$ activity, a matrix of supports was prepared with various ratios of γ-Al$_2$O$_3$, CBV-2314, and TiO$_2$ and loaded with 0.2 wt% Pd. Table 6 separates the composition of the supports into three categories of either ascending or descending amounts of γ-Al$_2$O$_3$, CBV-2314, and TiO$_2$ and the overall NO$_x$ conversion for each catalyst that was obtained from the calculation of the area under the NO$_x$ curve from 100 to 550 °C. The Pd/(60+20)−20 catalyst was used as a comparison benchmark. The DeNO$_x$ activity and N$_2$ selectivity as a function of support composition were compared for the catalysts in each category.

Figure 1 shows the NO$_x$ conversion and N$_2$ selectivity of the catalysts in the first category. All the NO$_x$ conversion curves were similar; however, catalyst activity declined as the zeolite content increased and the TiO$_2$ content decreased. The SAs of these catalysts (Table 5) were similar (ca. 271 to 297 m²/g), suggesting that the difference in activity was related to the support composition. The Pd/(60+30)−10 catalyst had the highest SA of this series but the overall lowest activity. These data confirmed that the support composition had a more pronounced effect on the activity of the catalyst than the SA.

Figure 2 shows the activity and selectivity of the catalysts in the second category. In this case, as the CBV-2314 content decreased, there was a change in the DeNO$_x$ activity curve between 160 and 200 °C. The NO$_x$ conversion slightly decreased as the CBV-2314 content was reduced and was significantly affected (less than 20 % NO$_x$ conversion between 160 and 200 °C) for the Pd/(80+0)−20 sample. These data suggest that the DeNO$_x$ activity near 180 °C is related to the amount of zeolite present in the support. However, the activity near 150 °C remains nearly identical for the three catalysts,

Table 6 Matrix and overall NO$_x$ conversion of 0.2 wt% Pd catalysts prepared with varying ratios of γ-Al$_2$O$_3$, CBV-2314, and TiO$_2$

γ-Al$_2$O$_3$ (wt%)	CBV-2314	TiO$_2$	Overall NO$_x$ conversion[a] (%)
60	20	20	24.6
60	25	15	20.7
60	30	10	18.6
65	15	20	21.5
70	10	20	21.6
80	0	20	18.3
50	30	20	19.0
0	80	20	20.3

[a] Value obtained from the calculation of the area under the NO$_x$ curve from 100 to 550 °C
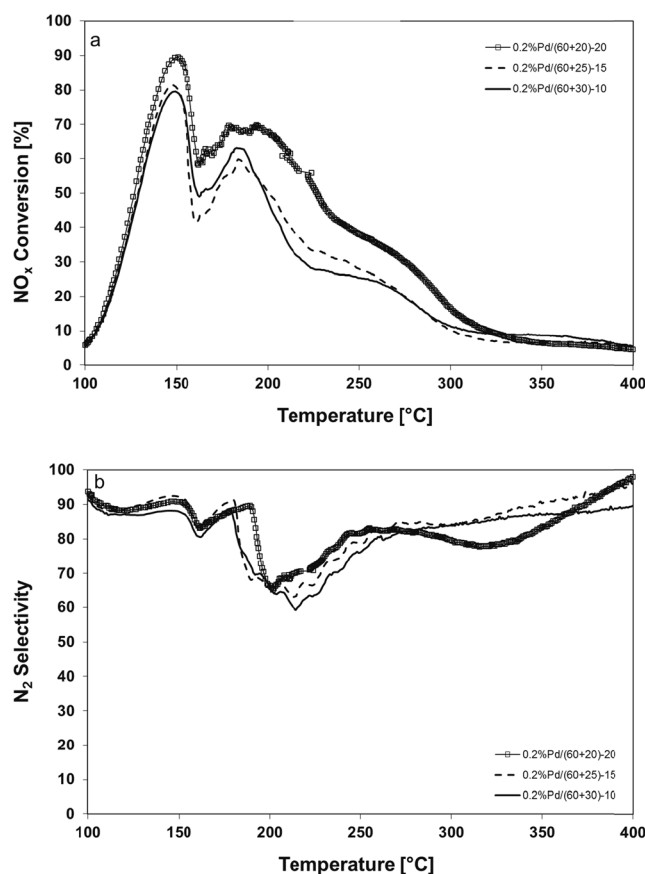
Fig. 1 Comparison of NO$_x$ conversion (**a**) and N$_2$ selectivity (**b**) of 0.2 %Pd(60+20)−20, 0.2 %Pd(60+25)−15, and 0.2 %Pd(60+30)−10 catalysts
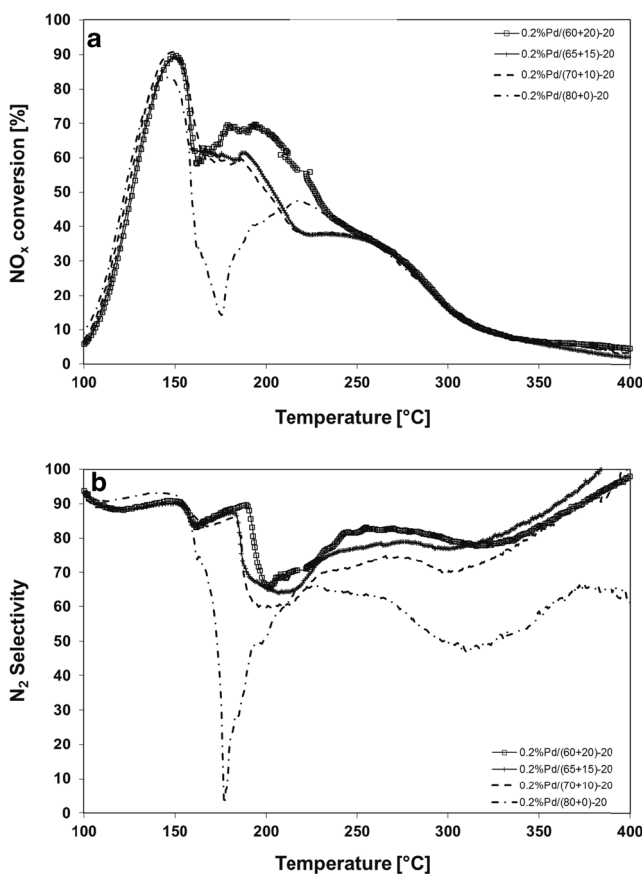
Fig. 2 Comparison of NO_x conversion (a) and N_2 selectivity (b) of 0.2 %Pd(60+20)−20, 0.2 %Pd(65+15)−20, 0.2 %Pd(70+10)−20, and 0.2 %Pd(80+0)−20 catalysts

suggesting that the zeolite content does not affect the activity at this temperature.

As the γ-Al_2O_3 content decreased, the activity near 150 °C decreased (Fig. 3) and was almost non-existent in the Pd/(0+80)−20 sample which contained no γ-Al_2O_3. The N_2 selectivity curves for most of the catalysts approached 90 % in the temperature range 100–180 °C then dropped to approximately 60 % in the 180–250 °C range and subsequently increased to approximately 90 % for the remainder of the run.

It is expected that the $DeNO_x$ reaction mechanism of the catalysts in this study is similar to the one described by Macleod et al. [30] due to their comparable formulations. According to the mentioned mechanism, in the low-temperature region (100–150 °C), the catalysts, in the presence of a stream containing $NO/CO/H_2/O_2$, formed isocyanates (NCO) in situ that were quickly hydrolyzed into NH_3 which subsequently reduces NO_x. There was apparently a synergy between TiO_2 and Al_2O_3 that results in promoting the formation of isocyanate on Pd located in proximity to both oxides. Furthermore, the Al_2O_3 phase was shown to increase the rate of NCO hydrolysis into NH_3. The authors suggested that the high-temperature mechanism (>200 °C) involved Pd/TiO_2 component of
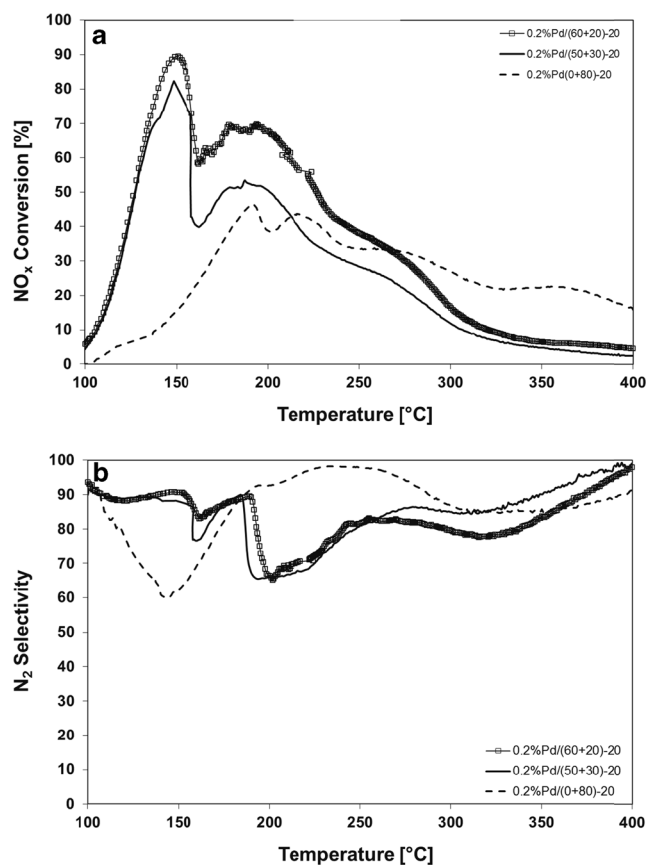

Fig. 3 Comparison of NO_x conversion (a) and N_2 selectivity (b): 0.2 %Pd(60+20)−20, 0.2 %Pd(50+30)−20, and 0.2 %Pd(0+80)−20

the catalyst for the formation of NH_3 directly from H_2 and NO, which in turn reduced NO_x. The reaction channel in this range did not involve the use of CO. In our study, the catalysts also showed additional significant activity in the medium-temperature region (160–200 °C). The activity in this region may be attributed to the presence of CBV-2314 component in the catalyst. The NO_x reduction mechanism of the catalysts with CBV-2314 was likely to be the same as in the low-temperature region (<150 °C) since alumina is a part of
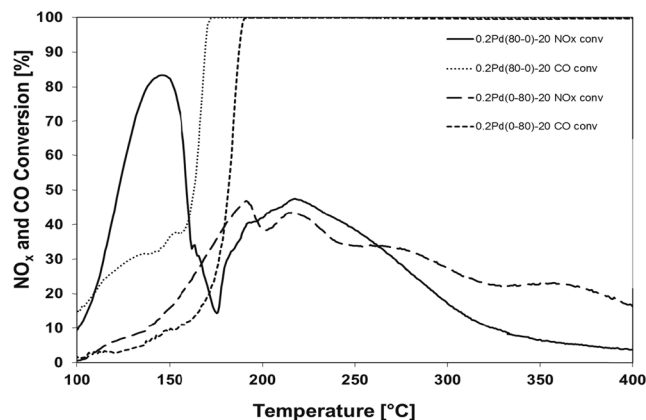

Fig. 4 NO_x conversion and CO light-off curves of 0.2 %Pd/(80−0)−20 and 0.2 %Pd/(0−80)−20 catalysts
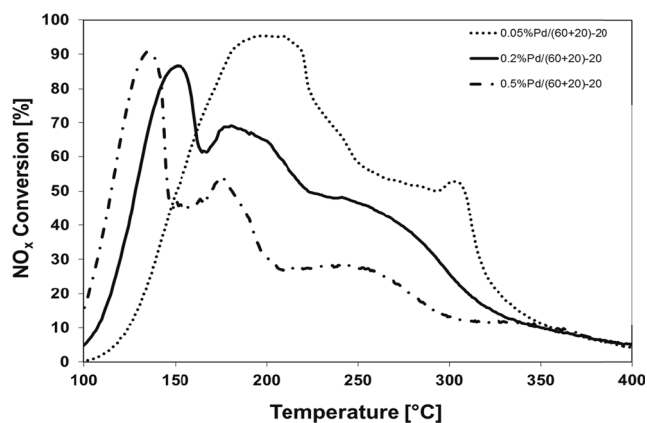
Fig. 5 NO$_x$ conversion of 0.05 wt% Pd (60+20)−20, 0.2 wt% Pd (60+20)−20 and 0.5 wt% Pd (60+20)−20 catalysts

Table 8 NO$_x$ light-off and overall NO$_x$ conversion of (60+20)−20 support loaded with various concentrations of Pd

Catalyst name	NO$_x$ light-off[a] (°C)	Overall NO$_x$ conversion (%)
0.05 wt% Pd/(60+20)−20	150	30.7
0.2 wt% Pd/(60+20)−20	127	24.6
0.5 wt% Pd/(60+20)−20	115	19.0

[a] Temperature at 50 % NO$_x$ conversion

(0.6 ppm or lower). This suggests that the ammonia formed in situ on the catalyst was almost entirely consumed for the reduction of NO$_x$, thus releasing no or very minute amounts of NH$_3$ slip in the exhaust.

3.3 DeNO$_x$ Activity of Catalysts with Various Loadings of Pd on (60+20)−20 Support

The (60+20)−20 support was loaded with various amounts of Pd in order to find the amount that would yield the optimum NO$_x$ conversion while minimizing the active metal content. Figure 5 shows the NO$_x$ conversion of the catalysts loaded with 0.05, 0.2, and 0.5 wt% Pd. The maximum NO$_x$ conversion shifted to higher temperature as the concentration of Pd
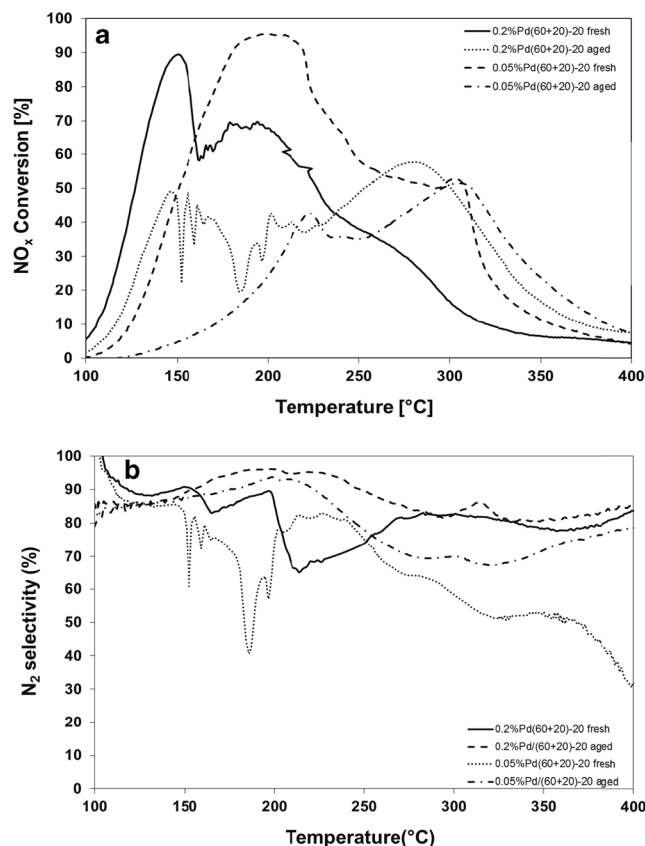
CBV-2314. Figure 4 provides insight as to why the catalysts with the zeolite were more active within the medium-temperature region compared to those without the zeolite. It shows the NO$_x$ conversion and the CO conversion of the Pd/(0−80)−20 (CBV-2314 + TiO$_2$) and the Pd/(80−0)−20 (Al$_2$O$_3$ + TiO$_2$) catalysts. For both catalysts, the CO conversion curves aligned with the NO$_x$ conversion curves. As the CO was converted, the NO$_x$ conversion increased and subsequently decreased when CO was completely consumed. The NO$_x$ conversion was especially low for Pd/(80−0)−20 when CO was completely converted since the formation of isocyanate without CO could not occur for the reaction to proceed. On the other hand, the CO conversion curve of the Pd/(0−80)−20 was shifted to higher temperature (with the associated rise in NO$_x$ conversion) compared to that of Pd/(80−0)−20. This result suggests that the CO conversion into NCO was slower on Pd/(0−80)−20 that may be caused by the higher concentration of silica in the catalyst. The hydrolysis of isocyanate is known to occur much less readily on silica than alumina [42, 43], and this may also be the cause of the slightly lower NO$_x$ conversion in this temperature region (160–200 °C) compared to the NO$_x$ conversion found in the low-temperature range (<150 °C). The highest overall NO$_x$ conversion (Table 6) of the Pd/(60+20)−20 amongst the catalyst series seems to be due to the optimum balance of Al$_2$O$_3$, CBV-2314, and TiO$_2$ oxides that provided the highest amount of NH$_3$ for reduction of NO$_x$.

For all catalysts, NH$_3$ was continuously monitored in the exhaust gas while testing for NO$_x$ reduction activity. In most cases, NH$_3$ was not detected or was near the detection limit

Table 7 Pd dispersion % on (60+20)−20 support

Pd nominal content (wt%)	Metal dispersion (%)
0.05	44.0
0.2	37.2
0.5	31.5

Fig. 6 NO$_x$ conversion (**a**) and N$_2$ selectivity (**b**) of 0.05 %Pd/(60−20)−20 and 0.2 %Pd/(60−20)−20 before and after aging
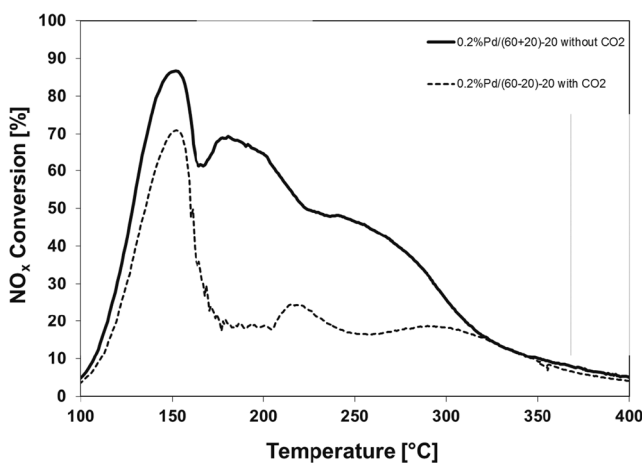
Fig. 7 NOx conversion of 0.2 %Pd/(60−20)−20 tested with and without CO₂

decreased. However, decreasing the Pd concentration increased the overall NOx conversion and the catalyst prepared with 0.05 wt% Pd obtained the widest temperature range of DeNOx activity. The N₂ selectivity was also high in the range of ~75 to 95 % (not shown) for each catalyst demonstrating the ability of these materials to obtain high NOx conversion and N₂ selectivity at low to medium temperatures. The high NOx conversion with low Pd content can be ascribed to the fact that as the loading of the metal decreases, the dispersion of the metal on the support, as shown in the Table 7. These results are in agreement with those reported by Law et al. [26].

While the 0.5 wt% Pd catalyst showed the earliest NOx light-off and the highest conversion at low temperature (90 % NOx conversion at 134 °C), it had much lower NOx conversion above 150 °C than the 0.05 wt%. Pd and 0.2 wt% Pd catalyst. Since the NOx light-offs for all three catalysts were determined to be low enough for most applications (equal to or below 150 °C, Table 8) and their N₂ selectivities were similar, the selection criterion of the best catalysts was based on the overall NOx conversion value that was calculated from the area under the NOx conversion curve from 100 to 550 °C. Table 8 shows the overall NOx conversion values for each catalyst. The 0.05 wt% Pd and the 0.2 wt% Pd catalyst exhibited the highest overall NOx conversion and were thus determined as the best candidates for further study.

3.4 Aged Catalysts

As the catalysts loaded with 0.05 wt% Pd and 0.2 wt% Pd on the (60+20)−20 support were identified as the best candidates, they were further investigated by conducting aging studies to establish their long-term stability.

Figure 6a, b shows the NOx conversion and N₂ selectivity, respectively, of the 0.2 wt% Pd/(60+20)−20 and 0.05 wt% Pd/(60+20)−20 catalysts tested before and after aging. The aging procedure simulated at least 80,000 km of on-road usage [44]. The maximum NOx conversion of 0.05 wt% Pd/ (60+20)−20 shifted to higher temperature and decreased from approximately 90 % at 200 °C to circa 51 % at 310 °C after aging. In addition, the overall DeNOx temperature activity range decreased for this catalyst. The NOx conversion temperature range of the 0.2 wt% Pd/(60+20)−20 broadened slightly after aging, and the NOx conversion near 150 °C was maintained but was reduced to approximately 50 %. The N₂ selectivity of both catalysts decreased after aging but was still above 50 % in the areas where significant NOx conversion occurred.

Table 9 gives the SA of the catalysts and the metal dispersion before and after aging. The SA of both catalyst decreased by approximately 40 %. Additionally, the metal dispersion of both catalysts decreased significantly. These results are indications that the decrease in SA and sintering of Pd cause the loss of activity for both catalysts.

3.5 Effect of CO₂ on Catalyst Activity

An additional activity test of the fresh 0.2 %Pd(60–20)−20 catalyst was performed using the regular simulated diesel exhaust composition with the addition of 7.5 vol% CO₂ to determine the effect of CO₂ on catalyst activity. This concentration of CO₂ was selected as the mid-point value of the typical range for diesel engine exhaust [45]. Figure 7 shows the comparison of the NOx conversion for the catalyst under regular simulated exhaust with and without CO₂. There was a slight increase in the NOx light-off temperature from 127 to 136 °C and a NOx conversion decrease of approximately 15 % at 151 °C when CO₂ was present. A more pronounced effect of CO₂ on the DeNOx activity was observed in the medium-temperature range of 180–300 °C (30–40 % decrease in NOx

Table 9 BET surface area of catalysts before and after aging

Catalyst name	BET surface area (m²/g)		Metal dispersion (%)	
	Before aging	After aging	Before aging	After aging
0.2 wt% Pd/(60+20)−20	290	161	37.1	20.8
0.05 wt% Pd/(60+20)−20	275	165	44.0	16.8

18

Emiss. Control Sci. Technol. (2016) 2:10–19

conversion). The results indicate that some improvements in DeNO$_x$ activity in the medium-temperature range are needed.

4 Conclusions

A series of ((H$_2$ + CO)-SCR DeNO$_x$ catalysts with Pd loaded on supports composed of various ratios of γ-Al$_2$O$_3$ and CBV-2314 coated with TiO$_2$ were successfully synthesized and tested for DeNO$_x$ activity. The catalysts showed high overall NO$_x$ conversions (50–90 %) in the 150–300 °C temperature range when tested using simulated diesel engine exhaust including water. The Pd-based catalyst with the support formulation of (60 wt% γ-Al$_2$O$_3$, 20 wt% CBV-2314, and 20 wt%TiO$_2$) demonstrated the highest overall NO$_x$ conversion that was attributed to the optimum balance of the three components forming the most NH$_3$ in situ for the reduction of NO$_x$. The comparison of three different concentrations of Pd (0.05 wt%, 0.2 wt%, and 0.5 wt%) on the (60 wt% γ-Al$_2$O$_3$, 20 wt% CBV-2314, and 20 wt%TiO$_2$) support composition revealed that the 0.05 wt% and 0.2 % wt% loading gave the optimal NO$_x$ conversion. These catalysts were further tested with accelerated aging, and the 0.2 wt% Pd/(60+20)−20 displayed the highest hydrothermal stability. The 0.2 wt% Pd/(60+20)−20 catalyst was also tested in the presence of CO$_2$ and showed some slight decrease in DeNO$_x$ activity in the low-temperature region, but more pronounced effect of CO$_2$ on activity was observed in the medium-temperature area. The study showed that the 0.2 wt% Pd/(60+20)−20 catalyst, with some improvements in the medium-temperature range, could be a good candidate as an ((H$_2$ + CO)-SCR DeNO$_x$ catalyst for low-temperature on-road and off-road applications.

References

1. Roy, S., Hegde, M.S., Madras, G.: Catalysis for NO$_x$ abatement. Appl. Energy **86**, 2283–2297 (2009)
2. Ligterink, N., de Lange, R., Vermeulen, R., Dekker, H.: On-road NO$_x$ emissions of Euro-V trucks. MON-RPT-033-DTS-2009-03840, (2009)
3. Furfori, S., Russo, N., Fino, D., Saracco, G.: NO SCR reduction by hydrogen generated in line on perovskite-type catalysts for automotive diesel exhaust gas treatment. Chem. Eng. Sci. **65**, 120–127 (2010). doi:10.1016/j.ces.2009.01.065
4. Mondragón Rodríguez, G.C., Kelm, K., Saruhan, B.: H$_2$-selective catalytic reduction of NO$_x$ activity and microstructural analysis of new BaTi$_{0.95}$Pd$_{0.05}$O$_3$ catalyst. Appl. Catal. A Gen. **387**, 173–184 (2010). doi:10.1016/j.apcata.2010.08.012
5. Mondragón Rodríguez, G.C., Saruhan, B.: Effect of Fe/Co-ratio on the phase composition of Pd-integrated perovskites and its H$_2$-SCR of NO$_x$ performance. Appl. Catal. B Environ. **93**, 304–313 (2010). doi:10.1016/j.apcatb.2009.10.004
6. Li, L., Wu, P., Yu, Q., Wu, G., Guan, N.: Low temperature H$_2$-SCR over platinum catalysts supported on Ti-containing MCM-41. Appl. Catal. B Environ. **94**, 254–262 (2010). doi:10.1016/j.apcatb.2009.11.016
7. Yu, Q., Kong, F., Li, L., Wu, G., Guan, N.: Fast catalytic reduction of NO$_x$ by H$_2$ over Pd-based catalysts. J. Catal. **31**, 261–263 (2010). doi:10.1016/S1872-2067(09)60045-0
8. Schott, F.J.P., Balle, P., Adler, J., Kureti, S.: Reduction of NO$_x$ by H$_2$ on Pt/WO$_3$/ZrO$_2$ catalysts in oxygen-rich exhaust. Appl. Catal. B Environ. **87**, 18–29 (2009)
9. Li, L., Zhang, F., Guan, N., Schreier, E., Richter, M.: NO selective reduction by hydrogen on potassium titanate supported palladium catalyst. Catal. Commun. **9**, 1827–1832 (2008). doi:10.1016/j.catcom.2008.02.019
10. Qi, G., Yang, R.T., Rinaldi, F.C.: Selective catalytic reduction of nitric oxide with hydrogen over Pd-based catalysts. J. Catal. **237**, 381–392 (2006). doi:10.1016/j.jcat.2005.11.025
11. Yang, J., Fu, O., Wu, D., Wang, S.: DRIFTS study of NO–H$_2$ reaction over Pd/Al$_2$O$_3$ with excess oxygen. Appl. Catal. B Environ. **49**, 61–65 (2004). doi:10.1016/j.apcatb.2003.11.017
12. Macleod, N., Lambert, R.M.: Selective NO$_x$ reduction during the H$_2$+NO+O$_2$ reaction under oxygen-rich conditions over Pd/V$_2$O$_5$/Al$_2$O$_3$: evidence for in situ ammonia generation. Appl. Catal. B Environ. **90**, 111–115 (2003)
13. Macleod, N., Cropley, R., Lambert, R.M.: Efficient reduction of NO$_x$ by H$_2$ under oxygen-rich conditions over Pd/TiO$_2$ catalysts: an *in situ* DRIFTS study. Catal. Lett. **86**, 69–75 (2003)
14. Burch, R., Coleman, M.D.: An investigation of promoter effects in the reduction of NO by H$_2$ under lean-burn conditions. J. Catal. **208**, 435–447 (2002)
15. Wen, B.: NO reduction with H$_2$ in the presence of excess O$_2$ over Pd/MFI catalyst. Fuel **81**, 1841–1846 (2002)
16. Costa, C.N., Stathopoulos, V.N., Belessi, V.C., Efstathiou, A.M.: An investigation of the NO/H$_2$/O$_2$ (lean-DeNO$_x$) reaction on a highly active and selective Pt/La$_{0.5}$Ce$_{0.5}$ MnO$_3$ catalyst. J. Catal. **197**, 350–364 (2001)
17. Machida, M., Ikeda, S., Kurogi, D., Kijima, T.: Low temperature catalytic NO$_x$-H$_2$ reactions over Pt/TiO$_2$-ZrO$_2$ in an excess oxygen. Appl. Catal. B Environ. **35**, 107–116 (2001)
18. Yang, J.I., Jung, H.: The effect of temperature on NO$_x$ reduction by H$_2$ in the presence of excess oxygen on a Pt/Al$_2$O$_3$ monolithic catalyst. Chem. Eng. J. **146**, 11–15 (2009)
19. Hong, Y., Lee, D., Ko, Y., Yinghua, L., Han, H., Lee, K.: Passive NO$_x$ reduction with CO using Pd/TiO$_2$/Al$_2$O$_3$+WGSR catalysts under simulated post-Euro IV diesel exhaust conditions. Catal. Lett. **136**, 106–115 (2010)
20. Nanba, T., Wada, K., Masukawa, S., Uchisawa, J., Obuchi, A.: Enhancement of activity of Ir catalysts for selective catalytic reduction of NO with CO by physical mixing with SiO$_2$. Appl. Catal. A Gen. **380**, 66–71 (2010). doi:10.1016/j.apcata.2010.03.028
21. Chen, J.C., Chang, F.Y., Wey, M.Y.: Modification of Pd/Al$_2$O$_3$ catalyst to improve the catalytic reduction of NO in waste incineration processes. Catal. Commun. **9**, 1106–1110 (2008)
22. Greenhalgh, B., Charland, J.-P., Stanciulescu, M., Burich, R., Kelly, J.: Pd-promoted catalysts for low temperature diesel engine DeNO$_x$. Catal. Today **151**, 285–290 (2010)
23. Li, Y., Lee, D., Hong, Y., Kim, S., Han, H., Lee, K.: Influence of Pd precursors on Pd/TiO$_2$/Al$_2$O$_3$ catalysts for lean NO$_x$ reduction with CO and H$_2$. React. Kinet. Mech. Catal. **99**, 361–369 (2010)
24. Kirillov, V.A., Smirnov, E.I., Amosov, Y., Bobrin, A.S., Belyaev, V.D., Sobyanin, V.A.: Reduction of nitrogen oxides in diesel

exhaust: prospects for use of synthesis gas. Kinet. Catal. **50**, 18–25 (2009)

25. Nakatsuji, T., Yamaguchi, T., Sato, N., Ohno, H.: A selective NO$_x$ reduction on Rh-based catalysts in lean conditions using CO as a main reductant. Appl. Catal. B Environ. **85**, 61–70 (2008). doi:10.1016/j.apcatb.2008.06.024

26. Law, H., Kung, M.C., Kung, H.H.: Low temperature NO$_x$ removal from diesel exhaust by coupling ethylene glycol reforming with SCR. Catal. Today **136**, 40–45 (2008). doi:10.1016/j.cattod.2007.11.060

27. Li, Y., Lee, D., Ko, Y., Hong, Y., Yoo, Y., Han, H., Lee, K.: NO$_x$ reduction with CO over supported Pd catalysts under simulated post Euro-IV diesel exhaust conditions. React. Kinet. Catal. Lett. **95**, 221–229 (2008)

28. Abu-Jrai, A., Tsolakis, A.: The effect of H$_2$ and CO on the selective catalytic reduction of NO$_x$ under real diesel engine exhaust conditions over Pt/Al$_2$O$_3$. Int. J. Hydrogen Energy **32**, 2073–2080 (2007)

29. Konsolakis, M., Vrontaki, M., Avgouropoulos, G., Ioannides, T., Yentekakis, I.V.: Novel doubly-promoted catalysts for the lean NO$_x$ reduction by H$_2$+CO: Pd(K)/Al$_2$O$_3$-(TiO$_2$). Appl. Catal. B Environ. **68**, 59–67 (2006)

30. Macleod, N., Cropley, R., Keel, J.M., Lambert, R.M.: Exploiting the synergy of titania and alumina in lean NO$_x$ reduction: in situ ammonia generation during the Pd/TiO$_2$/Al$_2$O$_3$ catalysed H$_2$/CO/NO/O$_2$ reaction. J. Catal. **221**, 20–31 (2004)

31. Lee, Y.W., Gulari, E.: Improved performance of NO$_x$ reduction by H$_2$ and CO over a Pd/Al$_2$O$_3$ catalyst at low temperatures under lean-burn conditions. Catal. Commun. **5**, 499–503 (2004)

32. Macleod, N., Lambert, R.M.: Lean NO$_x$ reduction with CO+H$_2$ mixtures over Pt/Al$_2$O$_3$ and Pd/ Al$_2$O$_3$ catalysts. Appl. Catal. B Environ. **35**, 269–279 (2002)

33. Macleod, N., Lambert, R.M.: Low-temperature NO$_x$ reduction with H$_2$+CO under oxygen-rich conditions over a Pd/ TiO$_2$/Al$_2$O$_3$ catalyst. Catal. Commun. **3**, 61–65 (2002)

34. Jobson, E.: Future challenges in automotive emission control. Top. Catal. **28**, 191–199 (2004)

35. Roy, S., Marimuthu, A., Hegde, M.S., Madras, G.: High rates of CO and hydrocarbon oxidation and NO reduction by CO over Ti$_{0.99}$Pd$_{0.01}$O$_{1.99}$. Appl. Catal. B Environ. **73**, 300–310 (2007)

36. Savva, P.G., Costa, C.N.: Hydrogen lean-DeNO$_x$ as an alternative to the ammonia and hydrocarbon selective catalytic reduction (SCR). Catal. Rev. Sci. Eng. **53**, 91–151 (2011). doi:10.1080/01614940.2011.557964

37. Macleod, N., Lambert, R.M.: An in situ DRIFTS study of efficient lean NO$_x$ reduction with H$_2$+CO over Pd/Al$_2$O$_3$: the key role of transient NCO formation in the subsequent generation of ammonia. Appl. Catal. B Environ. **46**, 483–495 (2003)

38. Macleod, N., Lambert, R.M.: In situ ammonia generation as a strategy for catalytic NO$_x$ reduction under oxygen rich conditions. Chem. Commun. **9**, 1300–1301 (2003)

39. Yan, D., Wang, H., Li, K., Wei, Y., Zhu, X., Cheng, X.: Structure and catalytic property of Ce$_{1-x}$Fe$_x$O$_2$ mixed oxide catalysts for low temperature soot combustion. Acta Phys. -Chim. Sin. **32**, 331–337 (2010)

40. Maunula, T., Kintaichi, Y., Inaba, M., Haneda, M., Sato, K., Hamada, H.: Enhanced activity of In and Ga-supported sol–gel alumina catalysts for NO reduction by hydrocarbons in lean conditions. Appl. Catal. B Environ. **15**, 291–304 (1998)

41. Shelef, M., Graham, G.W.: Why rhodium in automotive three-way catalysts? Catal. Rev. Sci. Eng. **36**, 433–457 (1994)

42. Dümpelmann, R., Cant, N.W., Trimm, D.L.: Formation of isocyanic acid during the reaction of mixtures of NO, CO and H$_2$ over supported platinum catalysts. Appl. Catal. B Environ. **6**, 291–296 (1995). doi:10.1016/0926-3373(95)00024-0

43. Dümpelmann, R., Cant, N.W., Trimm, D.L.: The formation of isocyanic acid (HNCO) by reaction of NO, CO, and H$_2$ over Pt/SiO$_2$ and its hydrolysis on alumina. J. Catal. **162**, 96–103 (1996). doi:10.1006/jcat.1996.0263

44. Komatsu, T., Tomokuni, K., Yamada, I.: Outstanding low temperature HC-SCR of NO$_x$ over platinum-group catalysts supported on mesoporous materials expecting diesel-auto emission regulation. Catal. Today **116**, 244–249 (2006). doi:10.1016/j.cattod.2006.01.035

45. Rajput, R.K.: In: A textbook of internal combustion engines, Laxmi publications, Bangalore, India, 537–611, (2005)